The Astrophysical Journal, 711:1229–1235, 2010 March 10 doi:10.1088/0004-637X/711/2/1229

FIVE LONG-PERIOD EXTRASOLAR PLANETS IN ECCENTRIC ORBITS FROM THE MAGELLAN PLANET SEARCH PROGRAM*

Pamela Arriagada[1], R. Paul Butler[2], Dante Minniti[1], Mercedes López-Morales[2,5], Stephen A. Shectman[3], Fred C. Adams[4], Alan P. Boss[2], and John E. Chambers[2]
[1] Department of Astronomy, Pontificia Universidad Católica de Chile, Casilla 306, Santiago 22, Chile; parriaga@astro.puc.cl
[2] Department of Terrestrial Magnetism, Carnegie of Washington, 5241 Broad Branch Road NW, Washington, DC 20015-1305, USA
[3] Carnegie Observatories, 813 Santa Barbara Street, Pasadena, CA 91101, USA
[4] Astronomy Department, University of Michigan, Ann Arbor, MI 48109, USA
Received 2009 June 10; accepted 2010 January 18; published 2010 February 23

ABSTRACT

Five new planets orbiting G and K dwarfs have emerged from the Magellan velocity survey. These companions are Jovian-mass planets in eccentric ($e \geqslant 0.24$) intermediate- and long-period orbits. HD 86226b orbits a solar metallicity G2 dwarf. The $M_P \sin i$ mass of the planet is 1.5 $M_{\rm JUP}$, the semimajor axis is 2.6 AU, and the eccentricity is 0.73. HD 129445b orbits a metal-rich G6 dwarf. The minimum mass of the planet is $M_P \sin i = 1.6\ M_{\rm JUP}$, the semimajor axis is 2.9 AU, and the eccentricity is 0.70. HD 164604b orbits a K2 dwarf. The $M_P \sin i$ mass is 2.7 $M_{\rm JUP}$, the semimajor axis is 1.3 AU, and the eccentricity is 0.24. HD 175167b orbits a metal-rich G5 star. The $M_P \sin i$ mass is 7.8 $M_{\rm JUP}$, the semimajor axis is 2.4 AU, and the eccentricity is 0.54. HD 152079b orbits a G6 dwarf. The $M_P \sin i$ mass of the planet is 3 $M_{\rm JUP}$, the semimajor axis is 3.2 AU, and the eccentricity is 0.60.

Key words: planetary systems – stars: individual (HD 86226, HD 129445, HD 164604, HD 175167, HD 152079)

Online-only material: color figures

1. INTRODUCTION

During the past 15 years, Doppler velocity surveys have uncovered more than 350 extrasolar planets around late F, G, K, and M stars within 100 pc. This planetary sample covers a wide variety of masses, orbital periods, and eccentricities (Butler et al. 2006; Udry & Santos 2007). Most of these planets are Jovian mass with semimajor axes less than 2 AU. Recent discoveries include Neptune-mass and terrestrial-mass planets with orbital periods of days to weeks (Rivera et al. 2005; Udry et al. 2006; Mayor et al. 2009; Vogt et al. 2010; Rivera et al. 2010), and solar system analogs with periods $\geqslant$10 yr (Jones et al. 2009; Marcy et al. 2002). While Doppler velocity surveys are increasingly oriented toward finding terrestrial-mass planets in small orbits, intermediate- and long-period companions around nearby stars continue to emerge, and are the primary targets for next generation imaging and interferometric missions.

Since planet formation and evolution theories were in the past based on our solar system, most planetary systems were expected to have circular or low eccentricity orbits. Instead, the observed range of exoplanet eccentricities ranges from 0 to 0.93, with a median of $e = 0.24$. The origin of exoplanet eccentricities remains as a basic, unanswered question for planet formation and evolution theory. Planets are believed to form on roughly circular orbits, necessitating a mechanism for pumping up their orbital eccentricities. Possible mechanisms include gravitational scattering by close encounters with other planets on crossing orbits (e.g., Weidenschilling & Marzari 1996; Rasio & Ford 1996), the Kozai (1962) mechanism, where orbital eccentricities and orbital inclinations can be interchanged in an oscillatory manner, and perturbations by other stars (Malmberg & Davies 2009). Disk torques during planet migration have also been advanced, though the eccentricity enhancements obtained are modest at best (e.g., Boss 2005; D'Angelo et al. 2006; Moorhead & Adams 2008). Recently, the Rossiter–McLaughlin effect has been used to determine high orbital inclinations in highly eccentric planets around binary systems (Winn et al. 2009a) as well as possible retrograde orbits (Winn et al. 2009b; Narita et al. 2009; Anderson et al. 2010). Understanding which dynamical interactions are responsible for these orbital peculiarities will require completing the census of exoplanet eccentricities and inclinations.

In this paper, we report the discovery of five eccentric Jupiter-mass planets from the Magellan Planet Search Program. To date the Magellan program has discovered 11 extrasolar planets, including the five reported here (López-Morales et al. 2008; Minniti et al. 2009).

2. THE MAGELLAN PLANET SEARCH PROGRAM

The Magellan Planet Search Program began taking data in 2002 December using the MIKE echelle spectrograph (Bernstein et al. 2003), mounted on the 6.5 m Magellan II (Clay) telescope located at Las Campanas Observatory in Chile. Using a 0.35 arcsec slit, MIKE obtains spectra with a resolution of $R \sim 50{,}000$, covering the wavelength range from 3900 to 6200 Å divided into a red and a blue CCD. An iodine absorption cell (Marcy & Butler 1992) is mounted in front of the MIKE entrance slit, imprinting the reference iodine spectrum directly on the incident starlight, providing a wavelength scale and a proxy for the spectrometer point-spread function (Butler et al. 1996). The iodine cell is a temperature-controlled sealed pyrex tube, such that the column density of iodine remains constant indefinitely.

The iodine spectrum (5000–6200 Å) falls on the red CCD. The blue CCD captures the Ca II H and K lines used to monitor stellar activity. We have monitored a number of stable main-sequence stars with spectral types ranging from late F to mid K.

* Based on observations obtained with the Magellan Telescopes, operated by the Carnegie Institution, Harvard University, University of Michigan, University of Arizona, and the Massachusetts Institute of Technology.
[5] Hubble Fellow.

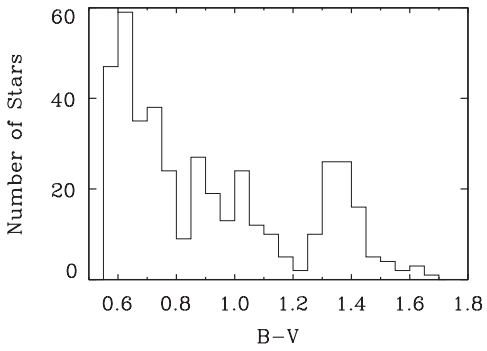

Figure 1. $B-V$ histogram of Magellan Planet Search Stars. The distribution peaks around Sun-like stars and diminishes for later spectral types. There is a secondary peak in the distribution around $B-V=1.35$, reflecting our bias toward adding the nearest M dwarfs.

Examples of these are shown in Figures 1 and 2 of Minniti et al. 2009. As these figures demonstrate, the Magellan/MIKE system currently achieves measurement precision of 5 m s^{-1}. The internal measurement uncertainty of our observations is typically 2–4 m s^{-1}, suggesting the Magellan/MIKE system suffers from systematic errors at the 3–4 m s^{-1} level. To account for this, the velocity uncertainties reported in this paper have 3 m s^{-1} is added in quadrature to the internally derived uncertainties.

The Magellan Planet Search Program is surveying ~400 stars ranging from F7 to M5. A histogram of the $B-V$ colors of the Magellan planet search stars is shown in Figure 1. Stars earlier than F7 do not contain enough Doppler information to achieve precision of 5 m s^{-1}, while stars later than M5 are too faint even for a 6.5 m telescope. The stars in the Magellan program have been chosen to minimize overlap with the AAT 3.9 m and Keck 10 m surveys. Subgiants have not been removed. Stellar jitter for subgiants is small, $\lesssim$5 m s^{-1} (Johnson et al. 2007). Stars more than 2 mag above the main sequence have much larger jitter, thus have been removed from the observing list based on *Hipparcos* distances (Perryman et al. 1997; ESA 1997).

Stars with known stellar companions within 2 arcsec are also removed from the observing list as it is operationally difficult to get an uncontaminated spectrum of a star with a nearby companion. Otherwise there is no bias against observing multiple stars. The Magellan target stars also contain no bias against brown dwarf companions or against metallicity.

3. HIGH-ECCENTRICITY JUPITER-MASS PLANETS FROM THE MAGELLAN SURVEY

This paper reports the discovery of five new planet-mass candidates. The stellar properties of the host stars are given in Table 1. The first two columns provide the HD catalog number and the *Hipparcos* catalog number, respectively. The stellar masses are taken from Allende Prieto & Lamber (1999), and [Fe/H] are taken from Holmberg et al. (2009). Spectral types are taken from the Simbad database.

Figure 2 shows the H line for the five stars reported in this paper, in ascending order of $B-V$. The Sun (bottom) is shown for comparison. Four of these stars are chromospherically quiet. The only star showing activity is the K2 dwarf HD 164604. Active K dwarfs have significantly lower radial-velocity "jitter" than F or G stars (Santos et al. 2000; Wright 2005). The expected photospheric radial-velocity jitter for all five of these stars is <3 m s^{-1}.

The best-fit orbital parameters of the companions are listed in Table 2. These are all massive planets with large signals

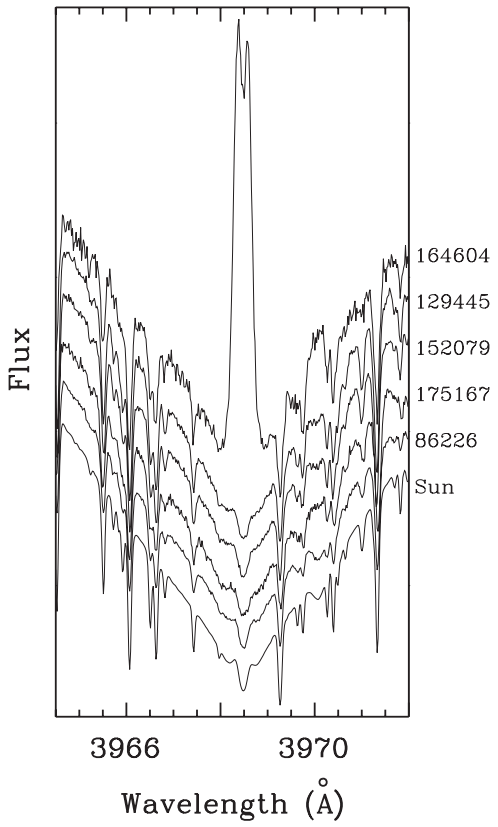

Figure 2. Ca II H line cores for the five target G dwarfs in the ascending order of $B-V$. The HD catalog number of each star is shown along the right edge. The Sun is shown for comparison.

Table 1
Stellar Properties

Star (HD)	Star (Hipp)	Spec Type	$M_{\rm Star}$ ($M_\odot$)	V (mag)	$B-V$	[Fe/H]	d (pc)
164604	88414	K2 V	0.8	9.7	1.39	−0.18	38
129445	72203	G6 V	0.99	8.8	0.756	0.25	67.61
86226	20723	G2 V	1.02	7.93	0.64	−0.04	42.48
175167	20723	G5 IV/V	1.102	8.01	0.751	0.19	67.02
152079	20723	G6 V	1.023	9.18	0.711	0.16	85.17

($K > 35$ m s^{-1}). Due to the sparseness of some of these data sets, the semi-amplitudes are poorly constrained. The uncertainties in the orbital parameters are calculated via a Monte Carlo approach as described in Marcy et al. (2005). The individual Magellan Doppler velocity measurements are listed in Tables 3–5. The properties of the host stars and of their companions are discussed in turn below.

3.1. HD 164604

HD 164604 is a K2 V dwarf with $V=9.7$ and $B-V=1.39$. The *Hipparcos* parallax (Perryman et al. 1997) gives a distance of 38.46 pc and an absolute visual magnitude $M_V=6.72$. Its metallicity is [Fe/H] = −0.18 (Holmberg et al. 2009).

Eighteen Magellan Doppler velocity observations of HD 164604 spanning 6 yr have been made, as shown in Figure 3 and listed in Table 3. The observations span three full orbital periods. The period of the best-fit Keplerian orbit is $P=1.66$ yr, the semi-amplitude is $K=77$ m s^{-1}, and the eccentricity is $e=0.24\pm0.14$. The rms of the velocity residuals to the Keplerian fit is 7.50 m s^{-1}. The reduced χ_ν of the Keplerian fit is 2.7.

Table 2
Orbital Parameters

Star (HD)	Period (days)	K (m s^{-1})	e	ω (deg)	T_0 (JD−2450000)	$M_P \sin i$ ($M_{\rm JUP}$)	a (AU)	$N_{\rm obs}$	rms (m s^{-1})
164604[a]	606.4 ± 9	77 ± 32	0.24 ± 0.14	51 ± 23	52674 ± 80	2.7 ± 1.3	1.3 ± 0.05	18	7.50
129445	1840 ± 55	38 ± 6	0.70 ± 0.10	163 ± 15	53093 ± 50	1.6 ± 0.6	2.9 ± 0.2	17	7.30
86226	1534 ± 280	37 ± 15	0.73 ± 0.21	58 ± 50	52240 ± 290	1.5 ± 1.0	2.6 ± 0.4	13	6.27
175167	1290 ± 22	161 ± 55	0.54 ± 0.09	342 ± 9	53598 ± 48	7.8 ± 3.5	2.4 ± 0.05	13	6.91
152079	2097 ± 930	58 ± 18	0.60 ± 0.24	325 ± 37	53193 ± 260	3.0 ± 2.0	3.2 ± 2.1	15	3.58

Note. [a] Additional velocity slope is -15.9 ± 2.9 m s^{-1} yr^{-1}.

Table 3
Velocities for HD 164604

JD (−2452000)	RV (m s^{-1})	Error (m s^{-1})
808.7659	−12.1	8.9
918.5317	−6.0	7.6
1130.9311	84.2	4.7
1540.7199	−34.7	3.8
2011.5059	−57.8	5.5
2013.5185	−63.0	4.8
2277.7380	−5.6	4.4
2299.6480	1.5	4.5
2300.6352	−9.1	4.5
2339.5686	21.3	4.8
2399.4832	55.2	4.6
2926.8545	−11.7	4.1
2963.8563	24.3	4.6
2965.8500	12.3	4.8
2993.7397	15.1	4.4
3001.7597	28.1	4.2
3017.7019	35.1	4.4
3019.7039	43.0	4.1

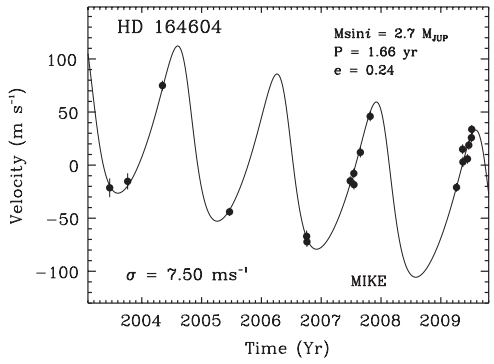

Figure 3. Doppler velocities for HD 164604 (K2 V). The solid line is a Keplerian orbital fit with a period of 1.66 yr, a semi-amplitude of 77.4 m s^{-1}, and an eccentricity of 0.24, yielding a minimum companion mass ($M_P \sin i$) of 2.7 $M_{\rm JUP}$. The rms of the Keplerian fit is 7.50 m s^{-1}. An additional linear trend of -15.9 m s^{-1} yr^{-1} provides evidence for a massive outer companion with a period greater than 7 yr and a semi-amplitude greater than 50 m s^{-1}.

Table 4
Velocities for HD 129445

JD (−2452000)	RV (m s^{-1})	Error (m s^{-1})
864.5311	26.1	8.2
1042.8730	−15.2	8.7
1127.8240	−35.8	4.2
1480.8541	15.7	5.7
1574.5786	22.5	4.8
1575.5511	29.4	4.4
1872.6777	43.7	4.2
2217.7257	33.3	4.3
2277.5928	37.5	4.8
2299.4993	31.6	4.3
2501.8506	44.2	4.1
2522.8417	32.9	4.4
2925.8091	−31.9	3.9
2963.7305	−40.3	4.2
2993.6537	−10.8	4.0
3001.6458	−21.4	4.2
3017.6200	−14.4	3.9

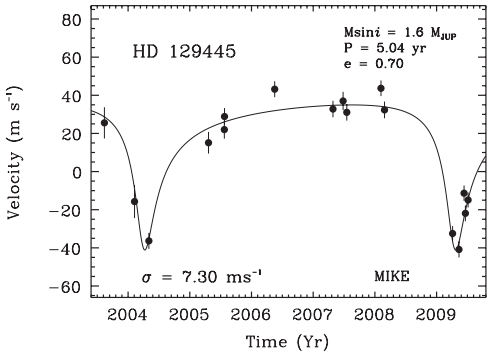

Figure 4. Doppler velocities for HD 129445 (G6 V). The solid line is a Keplerian orbital fit with a period of 5.04 yr, a semi-amplitude of 38 m s^{-1}, and an eccentricity of 0.70, yielding a minimum ($M_P \sin i$) companion mass of 1.6 $M_{\rm JUP}$. The rms of the Keplerian fit is 7.30 m s^{-1}.

Assuming a typical mass for a K2V star of $M_* = 0.8\,M_\odot$, the minimum mass of the companion is $M_P \sin i = 2.7\,M_{\rm JUP}$, and the orbital semimajor axis is 1.3 AU.

3.2. HD 129445

HD 129445 is a G6 V star with $V = 8.8$ and $B - V = 0.756$. The *Hipparcos* parallax (Perryman et al. 1997) gives a distance of 67.61 pc and an absolute visual magnitude, $M_V = 4.65$. Its metallicity is [Fe/H] = 0.25 (Holmberg et al. 2009).

Seventeen Magellan Doppler velocity observations of HD 129445 have been obtained, as shown in Figure 4 and listed in Table 4. The observations span a full orbital period. The semi-amplitude of the best-fit Keplerian orbit is $K = 38$ m s^{-1}, the period is $P = 5.04$ yr, and the eccentricity is $e = 0.70 \pm 0.10$. The rms of the velocity residuals to the Keplerian orbital fit is 7.30 m s^{-1}. The reduced χ_ν of the Keplerian orbital fit is 2.5. Assuming a stellar mass of $M_* = 0.99\,M_\odot$ (Allende Prieto & Lamber 1999), we derive a minimum mass of $M_P \sin i = 1.6\,M_{\rm JUP}$ and an orbital semimajor axis of 2.9 AU.

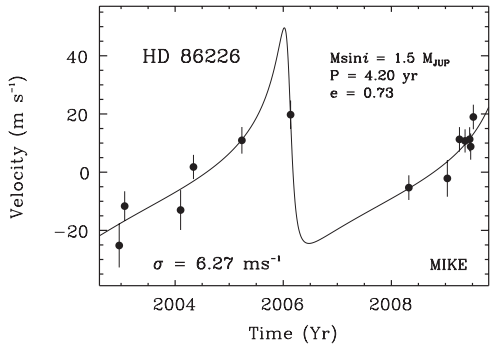

Figure 5. Doppler velocities for HD 86226 (G2 V). The solid line is a Keplerian orbital fit with a period of 4.20 yr, a semi-amplitude of 37 m s^{-1}, and an eccentricity of 0.73, yielding a minimum ($M_P \sin i$) of 1.5 M_{JUP} for the companion. The rms of the Keplerian fit is 6.27 m s^{-1}.

Table 5
Velocities for HD 86226

JD (−2452000)	RV (m s^{-1})	Error (m s^{-1})
626.8679	−24.6	7.5
663.7551	−11.1	5.1
1041.6735	−12.4	6.9
1128.5597	2.4	4.2
1455.6305	11.5	4.6
1784.7926	20.4	4.8
2583.6051	−4.7	4.2
2843.8112	−1.5	6.3
2925.6391	11.9	4.2
2963.5403	11.3	4.0
2994.5061	11.9	4.1
3001.4805	9.4	4.5
3019.4585	19.6	4.2

3.3. HD 86226

HD 86226 is a G2 V star with $V = 7.93$ and $B - V = 0.64$. The *Hipparcos* parallax (Perryman et al. 1997) gives a distance of 42.5 pc and an absolute visual magnitude, $M_V = 4.78$. Its metallicity is [Fe/H] = −0.04 (Holmberg et al. 2009).

Thirteen Magellan Doppler velocity observations have been made of HD 86226 over 6.5 yr, as shown in Figure 5 and listed in Table 5. These observations span a full orbital period. The best-fit Keplerian orbit to the Magellan data yields a period $P = 4.20$ yr, a semi-amplitude (K) of 37 m s^{-1}, and an eccentricity $e = 0.73 \pm 0.21$. The rms of the velocity residuals to the Keplerian orbital fit is 6.27 m s^{-1}. The reduced χ_ν of the Keplerian orbital fit is 1.82. Given the stellar mass $M_* = 1.02\ M_\odot$ (Allende Prieto & Lamber 1999), the minimum mass of the planet is $M_P \sin i = 1.5\ M_{JUP}$ with an orbital semimajor axis of 2.6 AU.

3.4. HD 175167

HD 175167 is a G5 IV/V star with $V = 8.01$ and $B - V = 0.75$. The *Hipparcos* parallax (Perryman et al. 1997) gives a distance of 67.02 pc and an absolute visual magnitude, $M_V = 3.88$, consistent with early evolution off the main sequence. Its metallicity is [Fe/H] = 0.19 (Holmberg et al. 2009).

Thirteen Magellan Doppler velocity observations have been made of HD 175167 spanning 5 yr, as shown in Figure 6 and listed in Table 6. These observations span a full orbital period. The best-fit Keplerian orbit to the Magellan data yields a period $P = 3.43$ yr, a semi-amplitude (K) of 161 m s^{-1}, and an eccentricity $e = 0.54 \pm 0.09$. The rms of the velocity residuals to the Keplerian orbital fit is 6.91 m s^{-1}. The reduced χ_ν of the Keplerian orbital fit is 2.7. Given the stellar mass $M_* = 1.102\ M_\odot$ (Allende Prieto & Lamber 1999), the minimum mass of the planet is $M_P \sin i = 7.8\ M_{JUP}$ with an orbital semimajor axis of 2.4 AU.

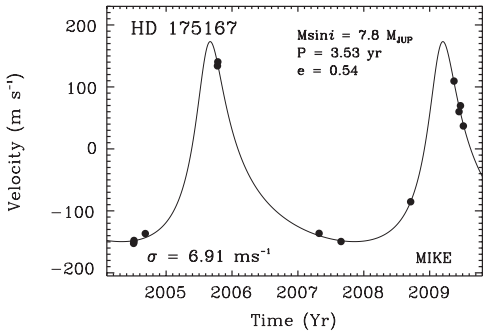

Figure 6. Doppler velocities for HD 175167 (G5 IV/V). The solid line is a Keplerian orbital fit with a period of 3.53 yr, a semi-amplitude of 161 m s^{-1}, and an eccentricity of 0.54, yielding a minimum ($M_P \sin i$) companion mass of 7.8 M_{JUP}. The rms of the Keplerian fit is 6.91 m s^{-1}.

Table 6
Velocities for HD 175167

JD (−2453000)	RV (m s^{-1})	Error (m s^{-1})
189.7359	−140.3	4.2
190.7340	−138.4	4.3
191.7523	−135.6	4.4
254.5236	−124.5	4.2
654.5074	146.1	4.3
656.5134	152.6	4.0
1217.9281	−124.1	4.5
1339.6070	−137.3	4.3
1725.6182	−73.1	3.8
1965.8675	121.6	4.2
1993.7656	72.3	4.1
2001.7759	81.9	4.3
2017.7389	49.1	3.9

3.5. HD 152079

HD 152079 is a G6 dwarf with $V = 9.18$ and $B - V = 0.71$. The *Hipparcos* parallax (Perryman et al. 1997) gives a distance of 85.17 pc and an absolute visual magnitude, $M_V = 4.53$. Its metallicity is [Fe/H] = 0.16 (Holmberg et al. 2009).

Fifteen Magellan Doppler velocity observations have been made of HD 152079 over 5.7 yr, as shown in Figure 7 and listed in Table 7. The best-fit Keplerian to the Magellan data yields a period $P = 5.7$ yr, a semi-amplitude (K) of 58 m s^{-1}, and an eccentricity $e = 0.60 \pm 0.24$. The rms of the velocity residuals to the Keplerian orbital fit is 3.58 m s^{-1}. The reduced χ_ν of the Keplerian orbital fit is 0.8. Given the stellar mass $M_* = 1.03\ M_\odot$ (Allende Prieto & Lamber 1999), the minimum ($M_P \sin i$) mass of the planet is $M_P \sin i = 3.0\ M_{Jup}$, with a semimajor axis of 3.2 AU.

4. DISCUSSION

This paper reports the detection of five companions using Magellan/MIKE that have not been previously published. These candidates are high-eccentricity long-period Jovian mass and larger planets orbiting nearby G and K dwarfs with metallicities ranging from [Fe/H] = −0.18 to [Fe/H] = 0.19.

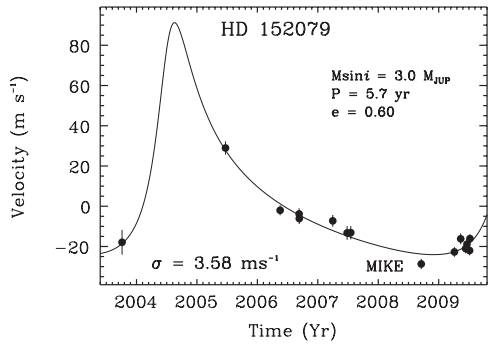

Figure 7. Doppler velocities for HD 152079 (G6 V). The solid line is a Keplerian orbital fit with a period of 5.04 yr, a semi-amplitude of 33.1 m s^{-1}, and an eccentricity of 0.56, yielding a minimum ($M_P \sin i$) of 3.0 M_{JUP} for the companion. The rms of the Keplerian fit is 3.58 m s^{-1}.

Table 7
Velocities for HD 152079

JD (−2452000)	RV (m s^{-1})	Error (m s^{-1})
917.4972	−24.3	6.2
1542.6649	22.5	3.3
1872.8022	−8.5	2.5
1987.5436	−10.3	2.8
1988.5202	−12.6	2.7
2190.8274	−13.7	2.9
2277.6950	−19.7	3.4
2299.6134	−19.6	3.3
2725.5353	−35.1	2.6
2925.9161	−29.2	2.4
2963.7753	−22.6	2.7
2993.7093	−27.5	2.4
3001.7291	−25.3	2.9
3017.6624	−28.5	2.4
3019.6938	−22.5	2.2

To date, there are 273 well-characterized known extrasolar planets, which show a wide range of eccentricities, from circular to about $e = 0.9$ with a median eccentricity of 0.24, in contrast to what was expected before the first exoplanets were discovered. Circular orbits in planets with $P < 20$ days can be explained by tidal circularization or orbit decay at periastron; however, the origin of the observed eccentricity distribution is still under debate. Currently, the most compelling explanation for the observed high eccentricities is that they result from planet–planet scattering interactions within systems that contain multiple companions. These interactions presumably take place after the epoch of planet formation, or perhaps during its latter stages. Scattering naturally produces large eccentricities much like the observed distribution, and often results in the ejection of planets (e.g., Moorhead & Adams 2005; Marzari 2005; Ford & Rasio 2008; Jurić & Tremaine 2008; Chatterjee et al. 2008). However, since planet–planet scattering alone cannot explain the observed distribution of semimajor axes (scattering cannot move planets far enough inward—Adams & Laughlin 2003), migration due to disk torques is also likely to take place. These disk torques can cause additional changes in eccentricity, including excitation (Goldreich & Sari 2003; Ogilvie & Lubow 2003), damping (e.g., Nelson et al. 2000), or both (Moorhead & Adams 2008). As a result, a complete explanation for the observed eccentricity distribution is still being constructed.

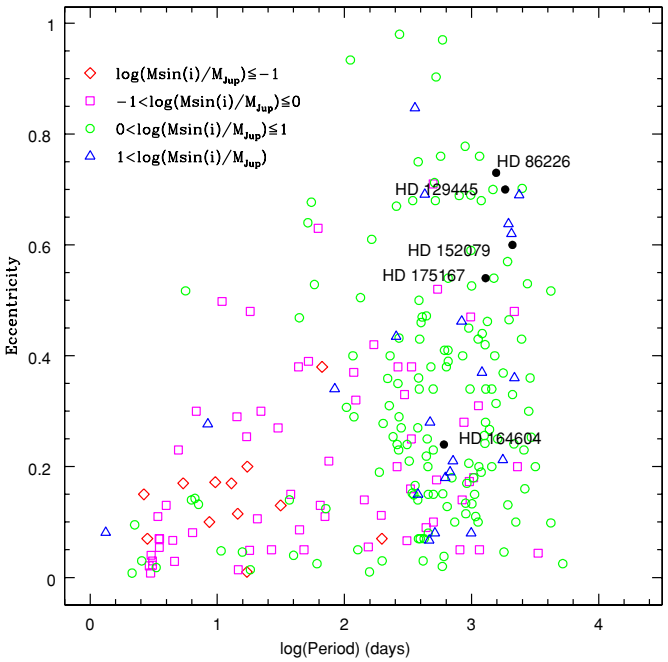

Figure 8. Eccentricities vs. orbital period of known extrasolar planets, where the planets reported in this paper are in filled symbols. Different symbols denote different mass ranges. Note that four of the planets announced in this paper have eccentricities higher than 0.5.

(A color version of this figure is available in the online journal.)

External bodies provide another source of perturbations that can affect orbital eccentricity, even in systems that have reached long-term stability. Such action can be driven by impulsive perturbations from passing stars in the birth cluster, or more gradually through distant stellar and/or massive planetary companions (Kozai 1962; Holman et al. 1997; Mazeh et al. 1997; Zakamska & Tremaine 2004; Malmberg & Davies 2009). Simulations of two-body interactions show how interactions between planets can lead to the observed eccentricity distribution (see Jurić & Tremaine 2008 and the aforementioned references). However, these simulations predict a slightly larger number of very eccentric ($e > 0.5$) planets than the observed distribution. On the other hand, Malmberg & Davies (2009) simulate planetary systems in binaries and study how the orbital elements can be affected by perturbations exerted by the second component; they find good agreement with the observed distribution of eccentricities for extrasolar planets with semimajor axes between 1 and 6 AU.

Our newly discovered candidates span eccentricities from 0.24 to 0.73, and semimajor axes from 1.3 to 3.2 AU. The parent stars of four of the candidates are not part of known binary systems, and their RV curves show no other low-mass companions. It is worth noting that in the period range $P > 1000$ days, there are 12 planets with eccentricities higher than 0.5, as shown in Figure 8. From these 12 planets, there is just one confirmed to be part of a binary system, and only three of them have eccentricities higher or similar to HD 129445, none of which belong to binary systems. Of the five planets reported in this paper, the lowest eccentricity value corresponds to HD 164604, the only candidate that shows a drift in velocity which indicates the presence of an additional outer body with an orbital period longer than 6 yr. In this case, the mechanism described by Malmberg & Davies (2009) could explain the planet's eccentricity. It is also worth noting that this planet

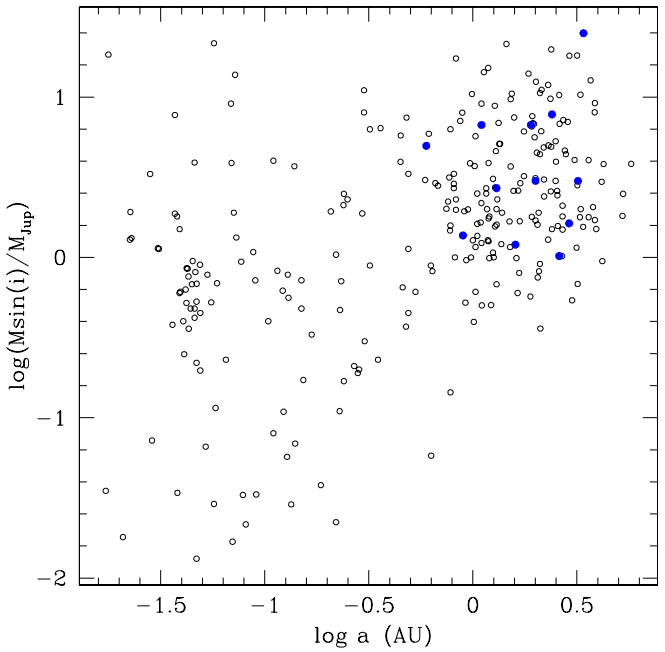

Figure 9. Semimajor axis (a) vs. $M \sin i$. All low-mass companions discovered by the Magellan Planet Search Program are highlighted as filled, blue circles. (A color version of this figure is available in the online journal.)

spends part of its orbit in the habitable zone of its parent star (∼0.9 AU). Ongoing discoveries and further characterization of long-period planets will lead to a better understanding of the origin of eccentric planet orbits.

To estimate the feasibility of performing an astrometric follow-up of our candidates, we have calculated their astrometric amplitude (218, 132, 117, 470, 168 μ arcseconds for HD164604, HD129445, HD 86226, HD 175167, and HD 152079, respectively). Ground-based surveys carried on CCD mosaic cameras mounted on medium-sized telescopes such as CAPSCam (Boss et al. 2009) can now achieve a precision of the order of milliarcsecond (mas), making it beyond the reach of the astrometric signature of our planetary companions from the ground with current technology. *Hipparcos* (Perryman et al. 1997) data provide positions with a precision of 1 mas for fairly bright stars and 0.5 mas for some stars after refinement (van Leeuwen 2007), which is still too low to detect such small signatures. To date, two of these amplitudes could only be reached using *Hubble Space Telescope* (*HST*) observations (Benedict et al. 2002; Benedict et al. 2008). In the future, however, optical space-based astrometric missions such as J-MAPS, *Gaia*, and *Space Interferometry Mission* will make possible to reach μas precision, making it plausible to observe such signature.

Imaging follow-up of our candidates with current ground-based 8 m class telescopes or *HST* would be just as unsuccessful. Due to the required magnitude contrast with the parent star, the minimum angular separation at which ∼5 $M_{\rm JUP}$ planets can be detected around solar-type stars is greater than 0.4 arcsec (Neuhäuser et al. 2005; Biller et al. 2007; Chun et al. 2008; Lagrange et al. 2009; Kasper et al. 2009), while these newly discovered planets, although long period, have angular separations of less than 0.1 arcsec, being too far to be reached by these instruments. They will be, however, main targets of next generation 30 m class telescopes equipped with adaptive optics and future interferometers.

These new planets clearly fit an emerging pattern that there is a dearth of planets with semimajor axes of less than ∼0.5 AU, as seen in Figure 9. Presumably, this is a signature of migration timescale versus formation timescale as a function of distance from the star, as suggested by Ida & Lin (2004).

We are grateful to the NIST atomic spectroscopy staff, in particular to Dr. Gillian Nave and Dr. Craig Sansonetti, for their expert oversight in calibrating our Iodine cell with the NIST FTS. R.P.B. gratefully acknowledges support from NASA OSS grant NNX07AR4OG. M.L.-M. acknowledges support provided by NASA through Hubble Fellowship grant HF-01210.01-A awarded by the STScI, which is operated by the AURA, Inc. for NASA, under contract NAS5-26555. D.M. and P.A. are supported by the Basal CATA PFB-06, FONDAP Center for Astrophysics 15010003, and FONDECYT 1090213. The referee, Dr. Michael Endl, made many helpful suggestions that significantly improved this paper. This paper has made use of the Simbad and NASA ADS databases.

REFERENCES

Adams, F. C., & Laughlin, G. 2003, Icarus, 163, 290
Allende Prieto, C., & Lamber, D. L. 1999, A&A, 352, 555
Anderson, D. R., et al. 2010, ApJ, 709, 159
Benedict, G. F., McArthur, B. E., & Bean, J. 2008, in IAU Symp. 248, A Giant Step: From Milli- to Micro-arcsecond Astrometry, ed. J. Wenjing (Dordrecht: Kluwer), 23
Benedict, G. F., et al. 2002, ApJ, 581, 115
Bernstein, R., Shectman, S. A., Gunnels, S. M., Mochnacki, S., & Athey, A. E. 2003, Proc. SPIE, 4841, 1694
Biller, B. A., et al. 2007, ApJS, 173, 143
Boss, A. P. 2005, ApJ, 629, 535
Boss, A. P., et al. 2009, PASP, 121, 1218
Butler, R. P., Marcy, G. W., Williams, E., McCarthy, C., Dosanjh, P., & Vogt, S. S. 1996, PASP, 108, 500
Butler, R. P., et al. 2006, ApJ, 646, 505
Chatterjee, S., Ford, E. B., Matsumura, S., & Rasio, F. A. 2008, ApJ, 686, 580
Chun, M., et al. 2008, Proc. SPIE, 7015, 49
D'Angelo, G., Lubow, S. H., & Bate, M. R. 2006, ApJ, 652, 1698
ESA 1997, The *Hipparcos* and *Tycho* Catalogues (ESA SP-1200; Noordwijk: ESA)
Ford, E. B., & Rasio, F. A. 2008, ApJ, 686, 621
Goldreich, P., & Sari, R. 2003, ApJ, 585, 1024
Holmberg, J., Nordström, B., & Andersen, J. 2009, A&A, 501, 941
Holman, M., Touma, J., & Tremaine, S. 1997, Nature, 386, 254
Ida, S., & Lin, D. N. C. 2004, ApJ, 604, 388
Johnson, J. A., et al. 2007, ApJ, 665, 785
Jones, H. R. A., et al. 2009, MNRAS, submitted
Jurić, M., & Tremaine, S. 2008, ApJ, 686, 603
Kasper, M., Amico, P., Pompei, E., Ageorges, N., Apai, D., Argomedo, J., Kornweibel, N., & Lidman, C. 2009, Msngr, 137, 8K
Kozai, Y. 1962, AJ, 67, 591
Lagrange, A.-M., et al. 2009, A&A, 493, 21
López-Morales, M., et al. 2008, AJ, 136, 1901
Malmberg, D., & Davies, M. B. 2009, MNRAS, 394, L26
Marcy, G. W., & Butler, R. P. 1992, PASP, 104, 270
Marcy, G. W., Butler, R. P., Fischer, D. A., Laughlin, G., Vogt, S. S., Henry, G. W., & Pourbaix, D. 2002, ApJ, 581, 1375
Marcy, G. W., Butler, R. P., Vogt, S. S., Fischer, D. A., Henry, G. W., Laughlin, G., Wright, J. T., & Johnson, J. A. 2005, ApJ, 619, 570
Marzari, F., Weidenschilling, S. J., Barbieri, M., & Granata, V. 2005, ApJ, 618, 502
Mayor, M., et al. 2009, A&A, 507, 487
Mazeh, T., Mayor, M., & Latham, D. W. 1997, ApJ, 478, 367
Minniti, D., Butler, R. P., López-Morales, M., Shectman, S. A., Adams, F. C., Arriagada, P., Boss, A. P., & Chambers, J. E. 2009, ApJ, 693, 1424
Moorhead, A. V., & Adams, F. C. 2005, Icarus, 178, 517
Moorhead, A. V., & Adams, F. C. 2008, Icarus, 193, 475
Narita, N., Sato, B., Hirano, T., & Tamura, M. 2009, PASJ, 61, 35
Nelson, R. P., Papaloizou, J. C. B., Masset, F., & Kley, W. 2000, MNRAS, 318, 18

Neuhäuser, R., Guenther, E. W., Wuchterl, G., Mugrauer, M., Bedalov, A., & Hauschildt, P. H. 2005, A&A, 435, L13
Ogilvie, G. I., & Lubow, S. H. 2003, ApJ, 587, 398
Perryman, M. A. C., et al. 1997, A&A, 323, L49 (The *Hipparcos* Catalog)
Rasio, F. A., & Ford, E. B. 1996, Science, 274, 954
Rivera, E., Butler, R. P., Vogt, S. S., Laughlin, G., Henry, G., & Mersciari, S. 2010, ApJ, 708, 1492
Rivera, E. J., et al. 2005, ApJ, 634, 625
Santos, N. C., Mayor, M., Naef, D., Pepe, F., Queloz, D., Udry, S., & Blecha, A. 2000, A&A, 361, 265
Udry, S., Mayor, M., Benz, W., Bertaux, J.-L., Bouchy, F., Lovis, C., Mordasini, C., Pepe, F., Queloz, D., & Sivan, J.-P. 2006, A&A, 447, 361
Udry, S., & Santos, N. C. 2007, ARA&A, 45, 397
van Leeuwen, F. 2007, A&A, 474, 653
Vogt, S. S., et al. 2010, ApJ, 708, 1366
Weidenschilling, S. J., & Marzari, F. 1996, Nature, 384, 619
Winn, J. N., et al. 2009a, ApJ, 703, 2091
Winn, J. N., et al. 2009b, ApJ, 703, L99
Wright, J. T. 2005, PASP, 117, 657
Zakamska, N. L., & Tremaine, S. 2004, AJ, 128, 869